(12) INTERNATIONAL APPLICATION PUBLISHED UNDER THE PATENT COOPERATION TREATY (PCT)

(54) Title: METHOD AND SYSTEM FOR REAL-TIME LENS FLARE RENDERING

Fig. 5
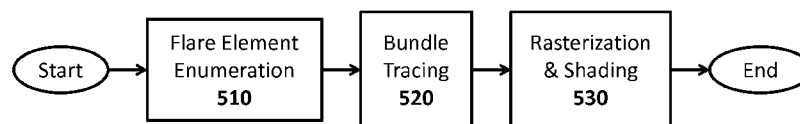
500

(57) Abstract: A method and device for efficiently simulating lens flares produced by an optical system is provided. The method comprises the steps of - Simulating paths of rays from a light source through the optical system, the rays representing light; and Es-timating, for points in a sensor plane, an irradiance, based on intersections of the simulated paths with the sensor plane.

METHOD AND SYSTEM FOR REAL-TIME LENS FLARE RENDERING

The present invention relates to a method and a system for real-time lens flare render-
ing.

TECHNICAL BACKGROUND

Lens flare is an effect caused by light passing through a photographic lens in any other
way than the one intended by design, most importantly through interreflection between
optical elements. Flare becomes most prominent when a small number of very bright
lights are present in a scene. In traditional photography and cinematography, lens flare
is considered a degrading artifact and therefore undesired. Among the measures to re-
duce flare in an optical system are optimized barrel designs, antireflective coatings,
and lens hoods.

On the other hand, flare or flare-like effects have often been used deliberately to
achieve an increase in realism or perceived dynamic range. Many image and video
editing packages feature filters for the generation of "flare" effects, and in video games
the effect is just as popular. In the production of computer-generated feature movies,
great effort has been taken to model cinema lenses with all their physical flaws and
limitations.

The problem of rendering lens flares has been approached from two ends. A very sim-
ple and efficient, but not quite accurate, technique is the use of static textures (star-
bursts, circles and rings) that move according to the position of the light source, and
are composited additively to the base image. Flares generated from texture billboards
can look convincing in many situations, yet they fail to capture the intricate dynamics
and variations of real lens flare.

On the other end of the scale, very sophisticated techniques have been demonstrated
that involve ray or path tracing through a virtual lens with all of its optical elements.
The results are near accurate but very costly to compute, with typical rendering times
in the order of several hours per frame on a current desktop computer. Furthermore,
many samples end up being blocked in the lens system, which wastes much of the
computation time and leads to a slow convergence. Also, the solution only holds with-
in the limits of geometric optics. Wave-optical effects, however, cause some pheno-
mena encountered in real lens flares. Integrating them into a ray-optical framework is
by no means trivial and further increases the computational cost.

PRIOR ART

Previous interactive methods are based on significant approximations. For example, it was suggested to use texture sprites that are blended into the framebuffer and arranged on a line through the screen center. Their position may be determined with an ad hoc displacement function. Size and opacity variation adapted by hand and depending on the angle between the light and camera have also been used. Additionally, a brightness variation of the flare has been proposed, that can also be controlled depending on the number of visible pixels of an area light. In none of these cases however, an underlying camera or lens model was considered.

In other situations, more accurate simulations are needed. For example, when compositing virtual and realistic content, when designing lens systems, or when predicting the appearance of a scene through a lens system. Previous high-quality approximations rely on path tracing or photon mapping. While such approaches deliver theoretically a high quality, several aspects; such as spectral (e.g., chromatic aberration, or lens coating), diffraction effects, or aperture shape, are usually ignored. Furthermore, the visual quality for small computation times can be insufficient, making interaction (e.g., zooming) impossible.

OBJECT OF THE INVENTION

It is therefore an object of the present invention to provide an improved method and system for efficiently rendering realistic lens flares.

SUMMARY OF THE INVENTION

This object is achieved by a method and a system according to the independent claims. Advantageous embodiments are defined in the dependent claims.

According to the invention, a method for simulating and rendering flares that are produced by a given optical system in real time may be based on tracing, i.e. on simulating, the paths of a select set of rays through the optical system and using the results of the simulation for estimating a point's irradiance in the film, i.e. sensor plane.

The invention provides a physically-based simulation that runs at interactive to real-time performance. Further, the inventive solution may be adapted to exaggerate or replace physical components. Its initial faithfulness ensures that the resulting imagery keeps a convincing and plausible appearance even after applying significant artistic tweaks.

3

BRIEF DESCRIPTION OF THE FIGURES

These and other aspects and advantages of the present invention may further be understood when reading the following detailed description of an embodiment of the invention, together with the annexed drawing, in which

FIG. 1   is a block diagram showing different aspects of optical systems considered by the invention.

FIG. 2   shows an example plot of the reflection coefficients for a quarter-wave coating, depending on a wavelength λ and an incident angle θ.

FIG. 3   shows an example transition of an octagonal aperture function from spatial to Fourier domain.

FIG. 4   shows a blade (a) and an aperture of an optical system (b).

FIG. 5   shows a flowchart of a method for simulating and rendering flares according to an embodiment of the invention.

FIG. 6   shows an example of a two-reflection sequence for an Itoh lens.

FIG. 7   shows the difference between intersecting rays with the nearest surface (a) and intersecting rays with a virtually extended lens surface according to an embodiment of the invention (b).

FIG. 8   shows a ray grid on the sensor plane, formed by the rays that have been traced through an optical system by the method described in connection with figure 5.

FIG. 9   shows performance ratings for an implementation of the method described in connection with figure 5, for different lens systems and quality settings.

DETAILED DESCRIPTION OF THE INVENTION

The main idea behind the inventive technique is not only to consider individual rays, but to exploit a strong coherence of rays within lens flare, in the sense of choosing rays underlying the same interactions with the optical system.

Figure 1 is a block diagram showing different aspects of optical systems considered by the invention. Generally, an optical system may comprise lenses and an aperture, each lens having a specific design, material and possibly, coating. Light propagation is governed by light transmission, and reflection at the set of lens surfaces and characteristic planes (entrance, aperture and sensor plane).

4

Specific lens designs of a given optical system may be modeled geometrically as a set of algebraically defined surfaces, i.e., spheres and planes. In terms of materials or optical media, it is sufficient for a method according to the present embodiment of the invention to consider perfect dielectrics with a real-valued refractive index. All optical glasses are dispersive media, i.e., the refractive index n is a function of the wavelength of light λ.

Sellmeier's empirical approximation may be used to describe the dispersion of optical glasses:

$$n^2(\lambda) = a + \frac{b\lambda^2}{c - \lambda^2} + \frac{d\lambda^2}{e - \lambda^2} + \frac{f\lambda^2}{g - \lambda^2} \qquad (1)$$

where $a, b, c, d, e, f,$ and g are material constants that can be obtained from manufacturer databases, e.g. an optical glass catalogue from Schott AG or from other sources, such as `http://refractiveindex.info`.

Every time a ray of light hits an interface between two different media, a part of it is reflected, and the rest transmitted. For smooth surfaces, it may be assumed that the relative amounts follow Fresnel's equations, with the resulting ray directions according to the law of reflection and Snell's law. The Fresnel equations provide different transmission and reflection coefficients for different states of polarization. For unpolarized light propagating from medium 1 to medium 2 (with refractive indices n_i and angles with respect to the normal θ_i), the overall reflection coefficient R and transmission coefficient T of a surface may be expressed as

$$R = \frac{1}{2}\left(\frac{n_1\cos\theta_1 - n_2\cos\theta_2}{n_1\cos\theta_1 + n_2\cos\theta_2}\right)^2 + \frac{1}{2}\left(\frac{n_1\cos\theta_2 - n_2\cos\theta_1}{n_1\cos\theta_2 + n_2\cos\theta_1}\right)^2 \qquad (2)$$

and $T = 1\text{-}R$.

However, in an attempt to minimize reflections, optical surfaces often feature antireflective coatings. They consist of layers of clear materials with different refractive index. Light waves that are reflected at different interfaces are superimposed and interfere with each other. In particular, if two reflections have opposite phase and identical amplitude, they cancel each other out, reducing the net reflectivity of the surface. The parameters of the multi-layer coatings used for high-end lenses are well-kept secrets of the manufacturers. But even the best available coatings are not perfect. A residual ref-

5

lectivity always remains. It is a function of wavelength and angle, $R(\lambda, \theta)$. Reflections in a coated surface therefore change color depending on the angle. Furthermore, a look into a real lens reveals that different interfaces reflect white light in different colors, suggesting that they are all coated differently. The resulting reflection residuals lead to

5   characteristic rainbow-colored lens flares.

Without the resources to reverse engineer exact characteristics, the inventors chose a so-called quarter-wave coating. It consists of a single thin layer. With this kind of coating, the reflectivity of the surface can be minimized for a center wavelength λ_0, given

10   an angle of incidence, θ_0. This requires a solid material of very low refractive index; in practice, the best choice is often M_gF_2 (n = 1.38). The layer thickness is chosen to result in a phase shift of $\pi/2$ (quarter period).

While an analytical expression for $R(\lambda, \theta)$ may be derived in most cases, even the sim-

15   ple quarter-wave coating involves multiple instances of the Fresnel equations, making the expression relatively complex. An example plot for a quarter-wave coating is shown in **figure 2**. One way to approximate such a function is to store it in a precomputed 2D texture, which also allows to record or use arbitrary available coating functions. In practice, the GPU's arithmetic power is usually high enough to evaluate

20   the function directly.

Appendix A shows an example of a computation scheme for the reflectivity $R(\lambda, \theta)$ of a surface coated with a single layer. The computation scheme also illustrates how polarization may be handled. Although an overall model of the optical system may assume

25   unpolarized light, the computation scheme of appendix A distinguishes between p- and s-polarized light, since light waves only interfere with other waves of the same polarization.

Some of the effects that constitute real lens flare cannot be explained in a purely geo-

30   metrical framework. As light waves traverse the optical systems, they are partially blocked by small-scale geometry (edges). The remaining parts of the wave front superimpose and form diffraction patterns. Exact computation of diffraction is expensive since it requires an integral over the transmission function for each image point. However, for the limit cases of near-field and far-field diffraction, the Fresnel and Fraunho-

35   fer approximations can be employed, respectively. Conveniently, both can be expressed in terms of Fourier transformations.

Far field (Fraunhofer): Up to a few factors for intensity and scaling (and potential non-linearities for large angles), the far-field amplitude distribution is proportional to the Fourier transformed transmission function. The size of the diffraction pattern is proportional to the wavelength, and its intensity must be scaled to preserve the overall power of the transmitted light.

For a given aperture function, plausible starbursts can be obtained by overlaying scaled copies of the aperture's FFT.

Near-Field (Fresnel): It has further been recognized by the optics community that, when the transformation from the spatial domain to the Fourier domain occurs through free-space propagation, intermediate field distributions of the diffracted wave can be obtained using the fractional Fourier transform (FrFT). The FrFT is a linear transformation that generalizes the standard Fourier transform to fractional powers, gradually rotating a signal from the spatial into the frequency domain. There exist various definitions of the FrFT based on propagation in graded-index media or the Wigner distribution functions, and they have been shown to be equivalent.

Figure 3 shows an example transition of an octagonal aperture function from spatial to Fourier domain. On the left-hand side, the aperture is transformed by 20%, while the right-hand side shows the transformation for a collection of different fractional powers.

However, in the inventive system, the assumption of free-space propagation does not hold. Computing the exact scalings and coefficients for diffraction patterns is not impossible, but hard due to the complexity of the optical system. By manually adjusting the few parameters, the look of real diffraction patterns may be closely reproduced.

Figure 4a shows the shape of an individual blade of an aperture. In real optical systems, the aperture consists of mechanical blades that control the size of a pupil by rotating into place. When the aperture is fully open, the blades are hidden in the lens barrel, resulting in a circular cross-section. Stopping down the aperture leads to a polygonal contour defined by number, shape and position of the blades.

Figure 4b shows the shape of an aperture. It may be simulated by combining multiple rotated copies of a base contour to form the proper aperture shape, which may be stored in a texture.

7

Depending on the requirements of the application, the above-described aspects may be skipped to simplify the model and increase the performance. They should rather be considered as building bricks that can either be modeled as accurately as desired, exaggerated, or altered in an artistically desired way.

Now, the rendering technique to simulate the actual light propagation will be described. It is based on ray tracing through the optical system to the film plane (sensor). In contrast to expensive off-line approaches, only a sparse set of rays may be traced. Each ray may record values about the lens-system traversal. When reaching the sensor, a ray corresponds to an image position. These rays implicitly define a ray grid across which the recorded values may be interpolated. Hereby, the outcome of rays may be approximated that were never actually shot, leading to an approximate beam tracing.

For the purpose of the following description, a directional, or distant, light source shall be assumed, which holds for most sources of flare (e.g., sunlight, street lights, and car headlamps). This assumption is not a necessary requirement of the inventive method, but helpful for its acceleration.

Figure 5 shows a flowchart of a method **500** for simulating and rendering flares according to an embodiment of the invention.

In **step 510**, lens flare elements are enumerated, based on a model of the optical systems as described above.

Rays traversing the lens system are reflected or refracted at lenses. Each flare element corresponds to a fixed sequence of these transmissions and reflections. An example of a two-reflection sequence for an Itoh lens is shown in **figure 6**. Sequences with more than two reflections may usually be ignored; only a small percentage of light is reflected and they are typically by orders of magnitude weakened leading to insignificant contributions in the final image.

Preferably, all two-reflection sequences are enumerated: light enters the lens barrel, propagates towards the sensor, is reflected at an optical surface, travels back, is again reflected, and, finally, reaches the sensor.

For n Fresnel interfaces in an optical system, there are $N = n(n - 1)/2$ such sequences that may be treated independently to produce their lens flare elements.

8

For a given flare element and incident light direction, a parallel bundle of rays is spanned by the entrance aperture of the lens barrel.

In **step 520**, a sparse set of rays is selected from each bundle for tracking their paths through the optical system. As the set of rays is associated with a flare element, it is uniform in the sense that the path of each ray through the optical system comprises a fixed number of reflections associated with the flare element. Because the sequence of the intersections is known for each flare element, unlike classical ray tracing, it is not necessary to follow each ray with a recursive scheme, elaborate intersection tests, or spatial acceleration structures. Instead, the sequence may be parsed into a deterministic order of intersection tests against the algebraically-defined lens surfaces. This makes the inventive technique particularly well suited for GPU execution.

At each intersection, the hitpoint of the ray may be compared with the diameter of the respective surface and it may be recorded, how far off a ray has been along its way through the system:

$$r_{rel}^{(new)} = \max(r_{rel}^{(old)}, r / r_{surface})$$

where r is the distance of the hitpoint to the optical axis, and $r_{surface}$ the radius of the optical element. Also, as a ray passes through the aperture plane, a pair of intersection coordinates (u_a, v_a) is stored.

Rays that escape from the system ($r_{rel} > 1$) must not be discarded since even these are valuable for interpolation in the ray grid (see below). For this purpose, lens surfaces may be extended virtually beyond their actual extent, as shown in **figure 7**. In fact, the lens functionality may be mathematically extrapolated beyond the lens diameter. All that is necessary is to keep the in-order treatment of the surface. Hereby, the numerical stability of the simulation is greatly increased, which would not be the case for standard ray tracing. This leads to more rays that pass through the system in a mathematically continuous way. Only when a ray can no longer be intersected with the next surface, or undergoes total internal reflection, it is pruned. Pruning can create holes in the ray grid, but refinement strategies are not needed. In practical trials by the inventors, it proved to be unproblematic because the rays transported energy approaches zero in the vicinity of total inner reflection, making its neighbors and the area on the ray grid appear black in the final rendering anyway.

In **step 530**, the final image in the sensor plane is obtained by rasterization and shading

9

Once the rays have been traced through the system, they form a ray grid on the sensor plane, as shown in **figure 8**. The set of rays is sparse and would only deliver insufficient quality. The objective is to interpolate information from neighboring rays to estimate the behavior of an entire ray beam. To this extent, rather than using a random sparse set of rays, the ray set may be initialized as a uniform grid placed at the first lens element. Each grid cell on the entrance plane may be matched to a grid cell on the sensor between the same rays. Similar to traditional beam tracing, the total radiant power transported through each beam is now distributed evenly over the area of the corresponding quad, leading to intensity variations in the lens flare. If a beam is focused on an area smaller than the beam's original diameter, the irradiance for that smaller area grows accordingly. Additional shading terms (in particular, Lambertian cosine terms) may be taken into account.

One important observation is that rays that are blocked are not culled by the lens system or aperture, but the position where they traverse the aperture (u_a, v_a), and its maximum distance to the optical axis, r_{rel}, with respect to the radius of the respective surface is recorded. When treating a beam, these coordinates may be interpolated over the corresponding quad. Hereby, more accurate inside/outside checks for the interpolated rays become possible; clipping is applied when the interpolated radius exceeds the limit distance. Finally, the position on the aperture may be used to determine the flare shape by a lookup in an aperture texture. Here, also Fresnel diffraction comes in, since the ringing pattern has been pre-computed and stored in the aperture texture.

In order to improve the speed and quality of the above described method and/or to save computational resources, the set of rays to be traced may be limited to a subset of rays that actually propagate all the way to the sensor, without hitting obstacles. In particular, for small aperture diameters, most rays are actually blocked in the aperture plane. According to the invention, the sparse set of rays may therefore be limited to a region on the entrance aperture that encloses all rays that might potentially hit the sensor. Hereby, the ray grid on the sensor will be concentrated around the actual lens flare element.

The bounding region on the entrance aperture depends on the light direction, aperture size, and possibly other parameters (zoom, or focus), making a run-time evaluation difficult. Instead, the invention proposes a preprocessing step to estimate the size and position of each lens flare.

10

For a given configuration, the previous basic algorithm may be employed with a low resolution grid to recover all rays that actually reach the sensor. Their position on the entrance aperture may then be used to define the bounding region, e.g. a rectangle. In theory, this solution might not be conservative, but, in practice, artifacts could be avoided with a simple solution. The derived bounding regions are extended slightly by taking the neighboring configurations into account. Preferably, a bounding rectangle may be determined that encompasses all bounding rectangles of the immediate neighbors which proved sufficient for all cases.

In practice, the process may further be improved by using an adaptive strategy instead of a brute-force sampling, e.g. by employing an interval subdivision guided by the variance in the bounding shape estimations.

In order to capture subtle changes introduced by specifics of the optical system, without sacrificing too much computational resources, the grid resolution for each flare element may be adapted at runtime. More specifically, lens flares may be considered as caustics of a complex optical system, which also implies that very high frequencies can occur. In the above-described embodiment of a method according to the invention, a regular grid of incident rays is mapped to a more or less homogeneous grid on the sensor. In most cases, the grid undergoes simple scaling and translation which is captured with sufficient precision even for a coarse tessellation. In some configurations, though, the accumulation of nonlinear effects may cause severe deformations, fold the grid onto itself, or even change its topology. Such flares require a higher grid resolution.

In order to adapt the grid resolution for each flare at runtime, a suitable heuristic may employ the area of grid cells as an indicator. A large variance across the grid implies that a non-uniform deformation occurred and more precision is needed. While one could always start with a small resolution, it is more efficient to initialize the grid resolution based on ratios that are measured from the ray bounding pre-computation. Based on variance, one out of six levels of detail may be used (with resolutions between 16×16 to 512×512 rays per bundle).

An approximate intensity of the resulting flare may also be derived during the pre-computation step. This allows sorting the flares according to their approximate intensity, i.e. their potential impact. A user may then control the budget, even during runtime, by fixing the number of flares to be evaluated.

11

In order to further increase the efficiency of the above-described method, rays travers-
ing the aperture twice may be disregarded. As these rays tend to be blocked anyhow,
their omission usually does not introduce strong artifacts. Hereby, the number of enu-
merated sequences may be reduced significantly to $N = (f(f - 1) + b(b - 1))/2$, where f
and b are the number of lens surfaces before and after the aperture respectively.

5

In order to reduce computational complexity, the above described embodiment of a
method according to the invention may also exploit symmetries in the optical system.
By design, most photographic lenses are axisymmetric, whereas anamorphic lenses
featuring two orthogonal planes of symmetry that intersect along the optical axis are
common in the film industry. For axial symmetry, the amount of required pre-
computation may be reduced drastically; all computation up to and including the ray
tracing may be done for a fixed azimuthal angle of incidence, and then rotated into
place. Furthermore, the sparse ray set may be reduced by exploiting the mirror symme-
try of the flare arrangement, only considering half the rays on the entrance plane. The
grid on the sensor may then be mirrored along the symmetry axis. Most notably, not
blocking rays directly, but recording aperture coordinates and intersection distances,
allows considering the whole system as symmetric (even the aperture, which, in gener-
al, is asymmetric).

10

15

20

Another gain in computational efficiency may be achieved by combining a reduction
in the number of wavelength-dependent evaluations with an interpolation strategy.
More particularly, treating antireflective coating and chromatic lens aberrations re-
quires a wavelength-dependent evaluation. For a brute-force evaluation, most flares are
well represented with only three wavelengths (RGB), but a few (typically, in extreme
cases, three out of 140 flares), can require up to 60 wavelengths for smooth results. In
an embodiment of the invention, the number of wavelengths may be limited to 3 (stan-
dard quality / RGB) or a maximum of 7 (high quality) wavelengths, implying only a
moderate computational cost. The result for a wavelength may be rendered and a filter
may be used in image space to create transitions. From the spatial variation between
neighboring wavelength bands, the orientation and dimension of the needed 1D blur
kernel may be determined per spectral flare. The filtered representations may then be
blended together in the RGBA frame buffer and deliver a smooth result.

25

30

Lens flare can also be a creative tool to increase the appeal of images. The inventive
algorithm offers many possibilities to interact with the basic pipeline in order to exceed
physical limitations while maintaining a plausible look. For example, the inventive
method does not make any assumptions concerning the aperture shape. Arbitrary defi-

35

12

nitions are possible, allowing indirect control of diffraction effects. Similarly, a user may draw the diffraction ringing and apply a Fourier transform to reconstitute the aperture. As the shape of the aperture appears also in form of ghosting, it may be interesting to handle both effects with differing definitions.

5

Moreover, lenses in the real world are often degraded by dust and imperfections on the surface that can affect the diffraction pattern. This effect may be controlled by adding a texture of dust and scratches to the aperture before determining the Fourier spectrum. Drawing a dirt texture is possible, but also a procedural generation of scratches and

10   dust may be offered based on user defined statistics (density, orientation, length, size). While scratches add new streaks to the lens flare, dust has a tendency to add rainbow-like effects. One particularly interesting possibility is to animate the texture and achieve dynamic glare.

15   Since real lens systems are also never exactly symmetric, real flare elements can be slightly off the mirror axis. To control this imperfection, a variance value can be added that translates each flare element slightly in the image plane. Such a direct modification is more intuitive than a corresponding change in the lens system.

20   Finally, in order to control color fringes of flares due to lens coating, a user may interactively provide color ramps or even global color changes for each flare.

The method according to the invention may be implemented on a computer. Preferably, the computer comprises a state-of-the-art graphics processing unit (GPU), because

25   the inventive method is well adapted to graphics hardware. More particularly, the ray tracing may be performed in a vertex shader of the GPU. The resulting distortion may be analyzed in the geometry shader and the energy may be adapted. Based on distortion, the pattern may be refined if needed. In modern graphics processing cards, this step may be executed by a tessellation unit. To deal with total reflection, culled rays

30   may be flagged via a texture coordinate, information that is then accessible to the geometry shader. The geometry shader produces the triangle strips that form the beam quads in the grid. For each quad the shading may be computed, taking the total radiant power into account. Furthermore, in case of a symmetric system, the sparse ray set may be halved and each triangle needs to be mirrored along the symmetry axis which

35   may be determined from the light position and the image center. This doubling of triangles is more efficient than image-based mirroring. The resulting quads on the sensor may be rasterized in the fragment shader that can discard fragments if they correspond to blocked rays, which is determined via a distance value. A texture lookup based on

the aperture coordinate may complete the final rendering in which all flares are com-
posited additively. An improvement in quality may be achieved by not shading quads,
but vertices. Then, the values may be interpolated in the fragment shader and deliver
smooth variations, as for Gouraud shading. At each vertex, the average value of its sur-
5   rounding neighbors may be stored. While accessing neighbor vertices is usually diffi-
cult, it is easy for a regular grid. To gain access to the vertices, they may be captured
via the transform feedback mechanism of modern hardware. Alternatively, a texture
may be written with the resulting values instead. In a second pass, the needed values
may simply be recovered per vertex by using easy-to-determine offsets.

10

In order to evaluate the above-described method, the inventors implemented it on an
Intel Core 2 Quad 2.83 GHz with an NVIDIA GTX 285 card. The method reaches in-
teractive to real-time frame rates depending on the complexity of the optical system,
and the accuracy of the simulation.

15

Therefore, it can be of interest for demanding real-time applications, but also for high-
er-quality simulations. For performance, one could even pick only those flares that are
particularly beautiful, yielding a significant speedup while maintaining the artistic ex-
pression. In practice, culling the 20% weakest flares using the inventive intensity LOD
20   delivers 20% speedup without introducing visible artifacts. Even 40% still proved ac-
ceptable for interactive applications (speedup approx. 50%).

Figure 9 shows performance ratings for different lens systems and quality settings.
Frames per second (Fps) are given for standard and high quality (more rays do not
25   bring improvement) settings. The most costly effects of the inventive method are caus-
tics in highly anisotropic flares because ray bundles in such flares are spatially and
spectrally incoherent.

The inventive solution performs a reasonably quick pre-computation step to bound the
30   sparse set of rays. For a simple lens, such as a Brendel prime lens (9 flares), it takes
less than 0.1 sec, for a Nikon zoom lens (142 flares), it takes 5 minutes, for the Canon
zoom lens (312 flares), it takes 20 min (all: flares $\times$ 90 light directions $\times$ 64^2 rays $\times$ 20
zoom factor $\times$ 8 aperture stops, the latter two allow to freely change camera settings on
the fly.

35

The inventive method produces physically-plausible lens flares. Most important effects
are simulated convincingly, leading to images that are hard to distinguish from real-
world footage. The main difference arises from imperfections of the lens system and

the approximate handling of diffraction effects according to the invention. Further-
more, the real lens coating is unknown, the invention works with an estimate.

The shape of the flare elements is rather faithfully captured. The inventive method
5   handles complex deformations and caustics (Fig. 15). Previous real-time methods were
unable to obtain similar results because ray paths were entirely ignored. Only costly
path tracing captured this effect, but did deliver a comparable quality in a reasonable
computation time. The inventive model considers many aspects that were previously
neglected (e.g., the reflectivity of lens coatings as a function of wavelength and angle).
10   Even with these improvements and at highest spatial and spectral resolutions, render-
ing flares for even the most complex optical designs takes no more than a few seconds.
This is significantly faster than a typical path-traced solution that would take hours, if
not days, to converge on today's desktop computers.

15   The memory consumption of the inventive approach is mainly defined by the textures
containing the aperture and its Fourier transform (24 MB worth of 16-bit float data), as
well as three render buffers (another 24 MB).

The inventive approach may be used in lens-system design to preview lens flare ap-
20   pearance, useful for manufacturers of lens systems. In particular, nowadays, an in-
creasing amount of designer-lens systems becomes available that exaggerate various
lens aberrations or similarly lens flares. Being able to predict such effects is particular-
ly interesting.

25   More particularly, the inventive technique delivers high quality that exceeds many
previous offline approaches, making it even interesting as a final rendering solution.
The added artistic control allows a user to maintain a realistic appearance while being
able to fine-tune the appearance.

30   In order to use the simulation in a computer game, costly calculations may be deacti-
vated. Furthermore, the two-reflection assumption allows the user to chose particular
flare elements considered important. Furthermore, for well-behaved flares, even a very
small amount of rays (for example 4 x 4) delivers high quality with the inventive inter-
polation,
35

The inventive methods are also useful in image and video processing. Current video
lens flare filters do not appear convincing because they keep a static look, e.g., flare
deformations are ignored. The inventive method is temporally coherent, making it a

good choice for movie footage as well. Light sources in the image may be detected and followed using an intensity threshold. One could also animate the light manually to emphasize elements or guide the observer. The instant feedback according to the invention is of great help in this context.

5

Finally, it must be noted that the invention is not limited to the embodiments previously discussed. More particularly, a rendering mechanism according to the invention may sample area light sources instead of approximating them by a point light, at an additional computational cost.

10

Appendix A: Single-Layer AR Coating

```
In:
        theta1(angle of incidence)
        lambda (wavelength)
        n1, n2 (refractive indices of media)
        nC, dC (refractive index and thickness of coating)
        // Typically for quarter wave coating;
        nC = max(sqrt(n1*n2),1.38),dC = lambda/4/nC

Out:
        R(reflectivity)

------------------------------------------------------------------

thetaC = asin(sin(theta1)*n1/nC);
theta2 = asin(sin(theta1)*n1/n2);

// amplitude for outer reflection/transmission on topmost interface.

rs1 = -sin(theta1 - thetaC)/sin(theta1 + thetaC);
rp1 =  tan(theta1 - thetaC)/tan(theta1 + thetaC);

ts1 = 2*sin(thetaC)*cos(theta1)/sin(theta1+thetaC);
tp1 = 2*sin(thetaC)*cos(theta1)/sin(theta1+thetaC)*cos(theta1+thetaC);

// amplitude for inner Fresnel reflection

rs2 = -sin(thetaC - theta2)/sin(thetaC + theta2);
rp2 =  tan(thetaC - theta2)/tan(thetaC + theta2);

//after passing through first surface twice two transmissions an one
reflection

ris = ts1^2*rs2;
rip = tp1^2*rp2;

// phase difference between outer and inner reflections

dy = dC*nC;
dx = tan(thetaC)*dy;
delay = sqrt(dx^2 + dy^2)
relPhase = 4*PI/lambda*(delay - dx*sin(theta1));

// optional: phase flip inf not (n0<n1<n2 || n0>n1>n2).
// Not needed for coatings of lower refractive index
// if (n1 > nC) relPhase += PI;
// if (nC > n2) relPhase += PI;

// Add sines of different phase and amplitude (trigonometrical identi-
ty)

out_s2 = rs01^2 + ris^2 + 2*rs1*ris*cos(relPhase);
out_p2 = rp01^2 + rip^2 + 2*rp1*rip*cos(relPhase);
R = (out_s2 + out_p2)/2;
```

5

CLAIMS

1. Method for simulating lens flares produced by an optical system, comprising the steps:

5

- simulating paths of rays from a light source through the optical system, the rays representing light;

- estimating, for points in a sensor plane, an irradiance, based on intersections of the simulated paths with the sensor plane.

10

2. Method according to claim 1, wherein the number of times a ray is reflected by a surface of the optical system, is fixed.

3. Method according to claim 2, wherein the fixed number of times is 2.

15

4. Method according to claim 1, wherein each ray's path passes through a bounded region of the entrance aperture of the optical system.

5. Method according to claim 4, wherein the bounds of the region are estimated in a

20   pre-processing step.

6. Method according to claim 1, further comprising the step of generating a digital image, based on the estimated irradiance.

25   7. Method according to claim 1, wherein the number of rays is sparse.

8. Method according to claim 1, wherein the number of rays is adapted at runtime.

9. Method according to claim 8, wherein the number of rays is adapted based on a

30   variance of the area of different cells formed by the intersections of the paths with the sensor plane.

10. Device for simulating lens flares produced by an optical system, comprising:

- means for simulating paths of rays from a light source through the optical
  system, the rays representing light;
- means for estimating, for points in a sensor plane, an irradiance, based on

5   intersections of the simulated paths with the sensor plane.

11. Device according to claim 10, wherein the means for simulating paths of rays is a
vertex shader of a graphics processing card.

10   12. Computer-readable medium storing a software that, when executed on a computer,
implements a method according to claim 1.

Fig. 1

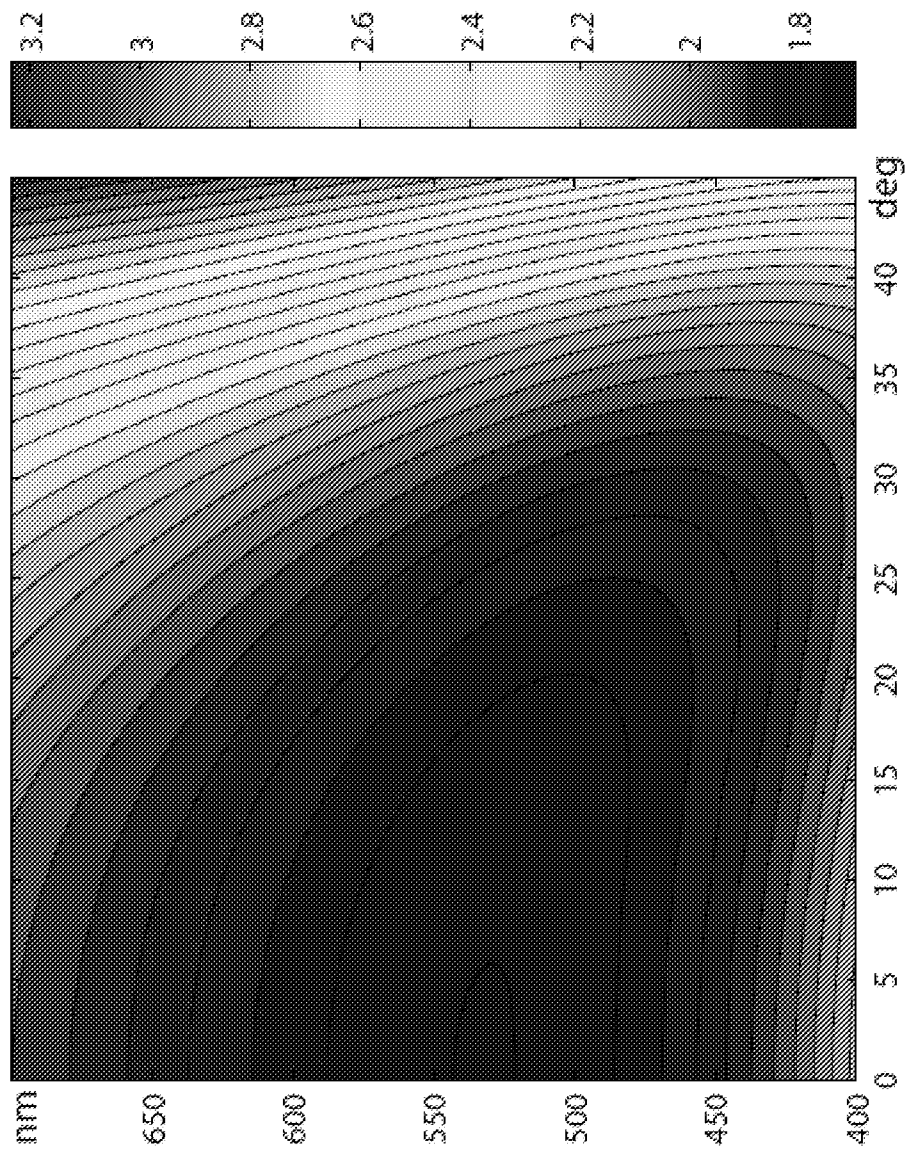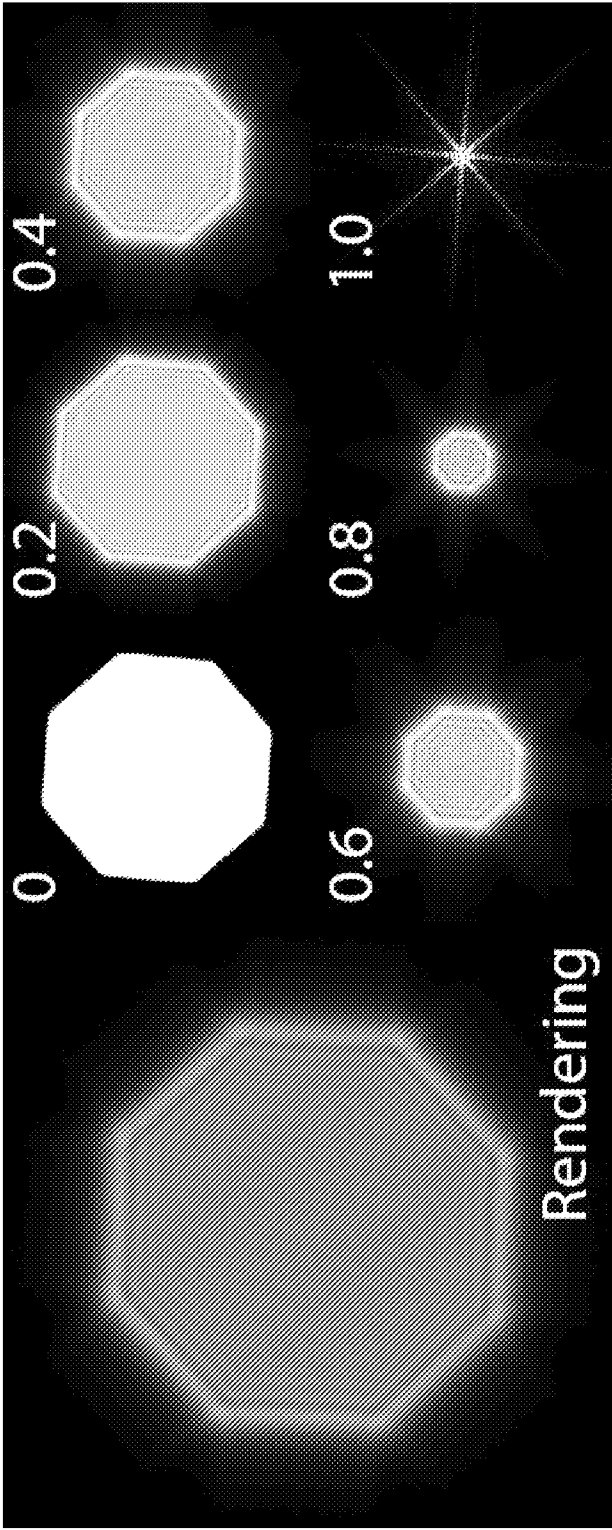| Optical System	Lens Design	Materials	Antireflective Coatings	Aperture
Light Transport	Dielectric Reflection / Transmission	Diffraction	Bounce Orders	Scaling Parameters
Implementation	Resolution / Sampling	Filtering: Textures, Spatial, Spectral		

Fig. 2

Effect of quarter-wave coating to reduce reflectivity for 532 nm light at normal incidence ($n_{glass} = 1.5$, $n_{coating} = 1.38$, $d = 96.4\,nm$).

Fig. 3

Fig. 4

Fig. 5

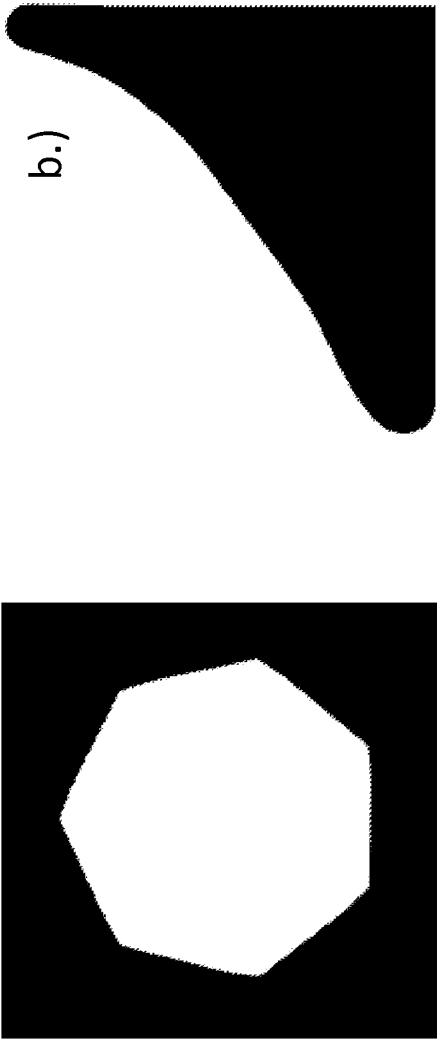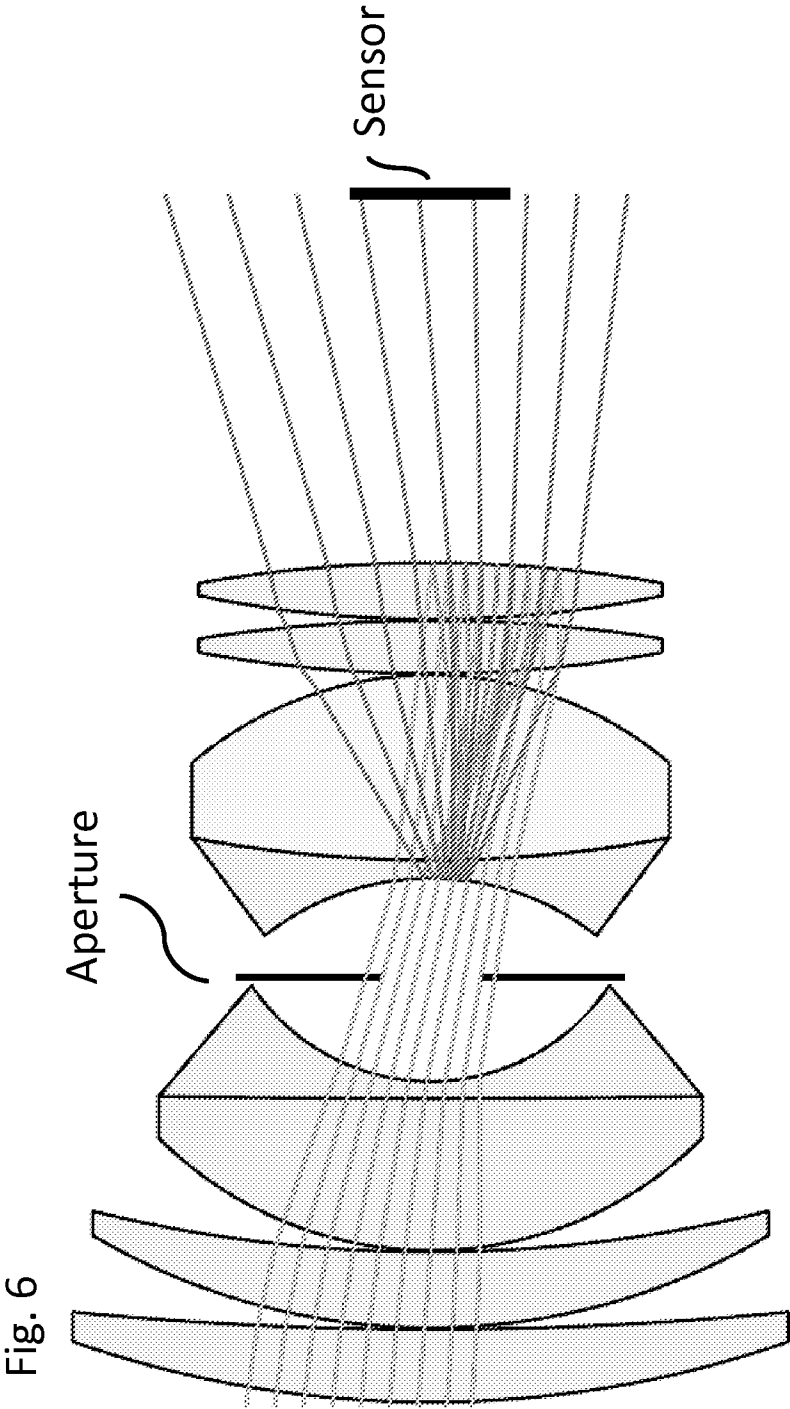Start → | Flare Element Enumeration **510** | → | Bundle Tracing **520** | → | Rasterization & Shading **530** | → End

500

Fig. 6

Fig. 7

a.)

Nearest-intersection

outer rays diverge

b.)

Fixed-intersection-order

outer rays converge
mathematically
continuous
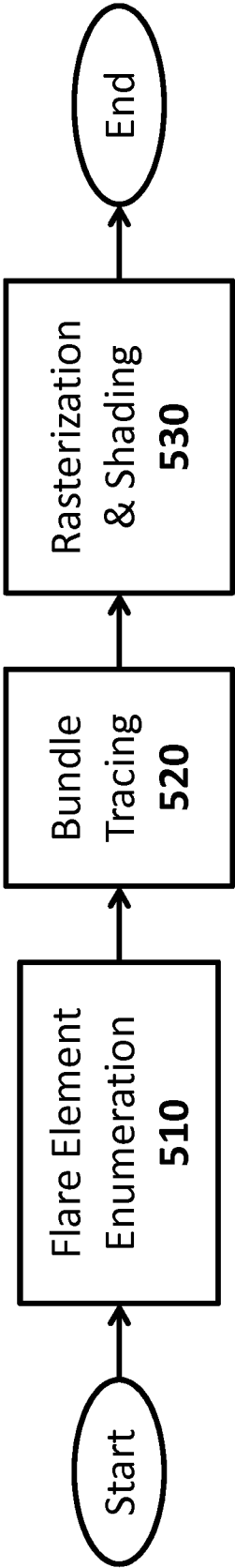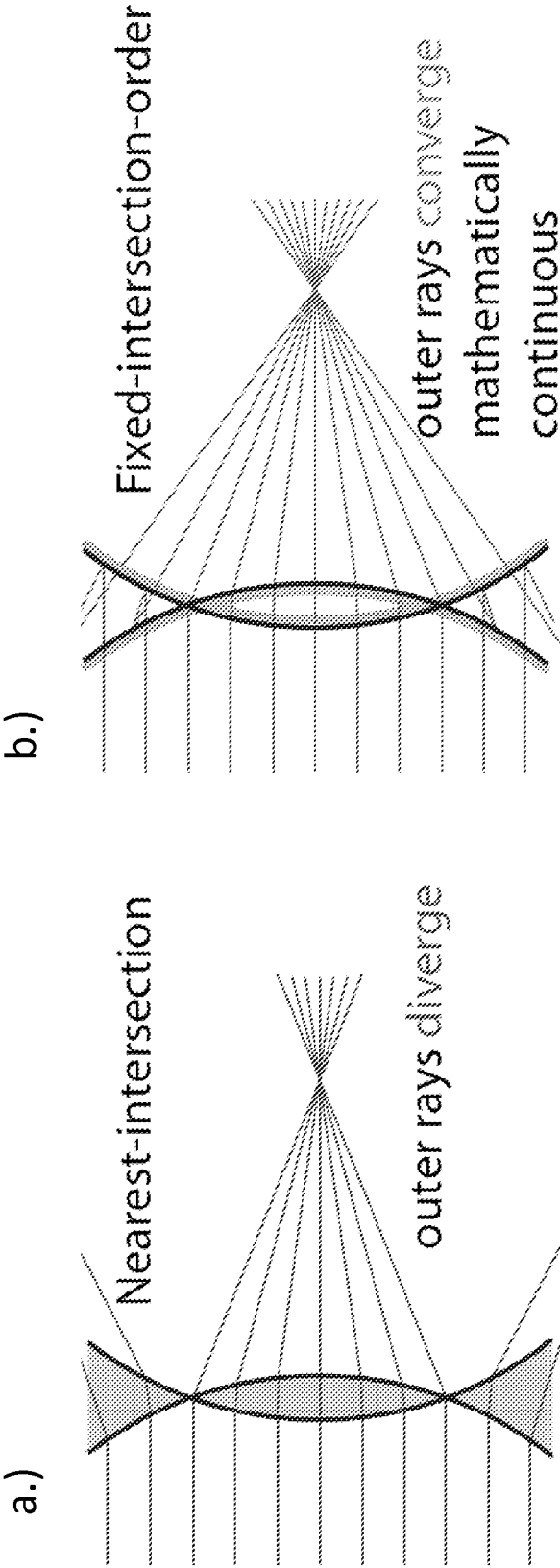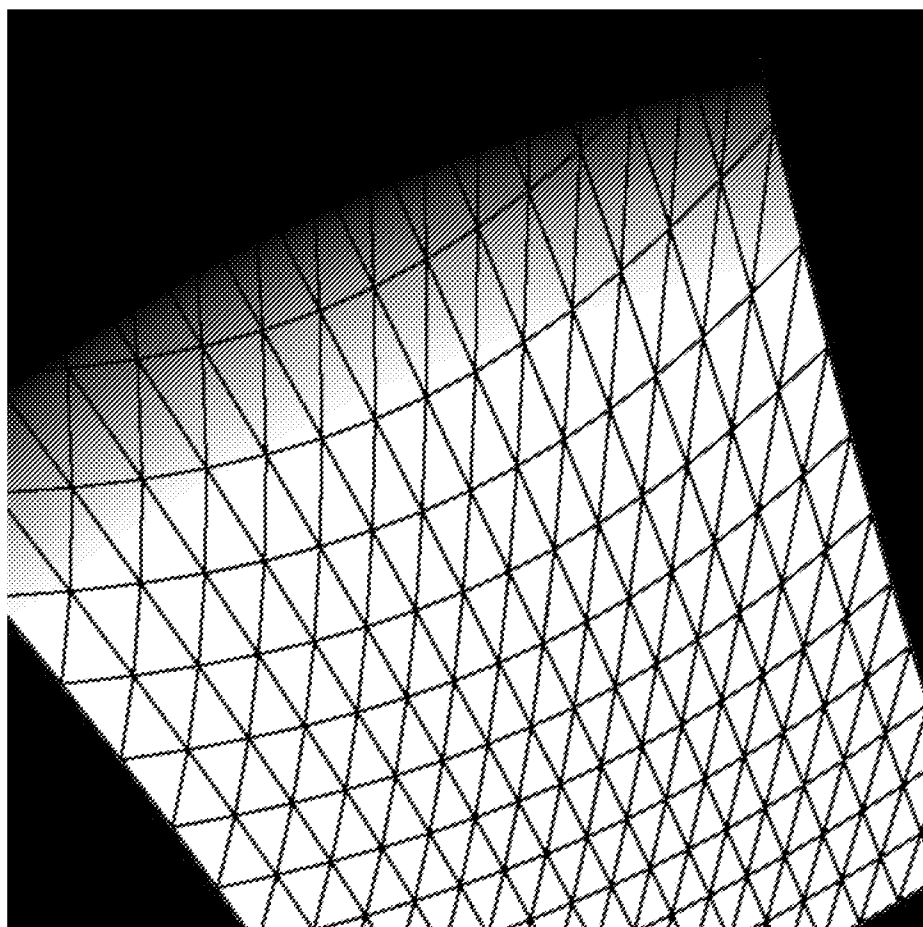
Fig. 8

Lens Layout	Lens System	Aperture fully open	Aperture reduced by 4 f-stops
	Canon EF 70–200mm f/2.8L	0.5/7.5 fps	0.7/9.5 fps
	Nikon 80–200mm f/2.8	1.2/23 fps	3.2/30 fps
	Itoh 100–145mm f/3.5	3.1/39 fps	8.6/47 fps
	Angenieux Biotar 100mm	1.8/58 fps	6.4/84 fps
	Kreitzer Tele 390mm f/5.6	7.7/110 fps	29/110 fps
	Brendel Tessar 100mm f/2.8	18/228 fps	21/189 fps

High Quality/Standard Setting

Fig. 9

INTERNATIONAL SEARCH REPORT

A. CLASSIFICATION OF SUBJECT MATTER
INV.   G06T15/50
ADD.   G06T17/10

According to International Patent Classification (IPC) or to both national classification and IPC

B. FIELDS SEARCHED

Minimum documentation searched (classification system followed by classification symbols)

G06T

Documentation searched other than minimum documentation to the extent that such documents are included in the fields searched

Electronic data base consulted during the international search (name of data base and, where practical, search terms used)

EPO-Internal, COMPENDEX, EMBASE, INSPEC, WPI Data

C. DOCUMENTS CONSIDERED TO BE RELEVANT

Category*	Citation of document, with indication, where appropriate, of the relevant passages	Relevant to claim No.
X	B. STEINERT ET AL: "General Spectral Camera Lens Simulation", COMPUTER GRAPHICS FORUM, vol. 30, no. 6, 1 March 2011 (2011-03-01), pages 1643-1654, XP55017414, ISSN: 0167-7055, DOI: 10.1111/j.1467-8659.2011.01851.x page 1643, line 1, paragraph 1. Introduction - line 17 page 1644, left-hand column, line 1, paragraph 2.1 Camera models - page 1644, left-hand column, line 10, paragraph 2.3 Full lens system page 1644, right-hand column, line 1, paragraph 2.5 Commercial engineering software - last line page 1645, right-hand column, paragraph 3.2 Glass interaction page 1647, left-hand column, line 1, -/--	1-12

|X| Further documents are listed in the continuation of Box C. |X| See patent family annex.

* Special categories of cited documents :

"A" document defining the general state of the art which is not considered to be of particular relevance

"E" earlier document but published on or after the international filing date

"L" document which may throw doubts on priority claim(s) or which is cited to establish the publication date of another citation or other special reason (as specified)

"O" document referring to an oral disclosure, use, exhibition or other means

"P" document published prior to the international filing date but later than the priority date claimed

"T" later document published after the international filing date or priority date and not in conflict with the application but cited to understand the principle or theory underlying the invention

"X" document of particular relevance; the claimed invention cannot be considered novel or cannot be considered to involve an inventive step when the document is taken alone

"Y" document of particular relevance; the claimed invention cannot be considered to involve an inventive step when the document is combined with one or more other such documents, such combination being obvious to a person skilled in the art.

"&" document member of the same patent family

Date of the actual completion of the international search	Date of mailing of the international search report
26 January 2012	03/02/2012

| Name and mailing address of the ISA/
 European Patent Office, P.B. 5818 Patentlaan 2
 NL - 2280 HV Rijswijk
 Tel. (+31-70) 340-2040,
 Fax: (+31-70) 340-3016 | Authorized officer

 Gauthier, J |

Form PCT/ISA/210 (second sheet) (April 2005)

C(Continuation).	DOCUMENTS CONSIDERED TO BE RELEVANT	
Category*	Citation of document, with indication, where appropriate, of the relevant passages	Relevant to claim No.
	paragraph 3.5.1 Flare effects - last line page 1647, right-hand column, line 1, paragraph 4. Full Lens System - page 1649, right-hand column, last line, paragraph 4.4 Aperture diffraction page 1650, right-hand column, line 1, paragraph 5.4 Lens Flare - right-hand column, last line, paragraph 5.5 Diffraction simulation figures 1,4,5,10,11,12,13 -----	
X	KOLB C ET AL: "A REALISTIC CAMERA MODEL FOR COMPUTER GRAPHICS", COMPUTER GRAPHICS PROCEEDINGS. LOS ANGELES, AUG. 6 - 11, 1995; [COMPUTER GRAPHICS PROCEEDINGS (SIGGRAPH)], NEW YORK, IEEE, US, 6 August 1995 (1995-08-06), pages 317-324, XP000546243, ISBN: 978-0-89791-701-8 abstract figures 1,2,4,6 page 318, left-hand column, line 4, paragraph 1. Introduction - last line page 318, left-hand column, line 4, paragraph 2. Lens System - page 319, right-hand column, last line, paragraph 3.1 Tracing Rays through Lens System page 320, right-hand column, line 1, paragraph 3.4 The Exit Pupil - last line page 322, left-hand column, line 1, paragraph 4.2 Sampling - right-hand column, line 11 ----- -/--	1,2,4-12

C(Continuation). DOCUMENTS CONSIDERED TO BE RELEVANT

Category*	Citation of document, with indication, where appropriate, of the relevant passages	Relevant to claim No.
X	MIKIO SHINYA ET AL: "RENDERING TECHNIQUES FOR TRANSPARENT OBJECTS", PROCEEDINGS/COMPTE RENDU GRAPHICS INTERFACE, XX, XX, 19 June 1989 (1989-06-19), pages 173-182, XP000957404, page 173, left-hand column, line 1, paragraph 1. Introduction - right-hand column, last line, paragraph 1. Introduction page 174, right-hand column, line 1, paragraph 2.2.2 Previous methods - page 176, right-hand column, line 8, paragraph 2.2.3 Grid-pencil tracing page 177, right-hand column, paragraph 2.3.2 Procedure page 178, left-hand column, line 1, paragraph 3. Pencil Tracing Dispersive Objects - page 179, left-hand column, last line, paragraph 3.2.2 Dispersion image solid page 180, left-hand column, line 1, paragraph 4. Cross-Screen Filter - line 17 page 180, right-hand column, line 1, paragraph 4.2 Implementation - page 181, left-hand column, last line figures 2,5,7,11,12,15 -----	1,2,4-12
A	SHINYA MIKIO: "Principles and Applications of Pencil Tracing", COMPUTER GRAPHICS, vol. 21, no. 4, 1 July 1987 (1987-07-01), pages 45-54, XP040129013, ACM, 2 PENN PLAZA, SUITE 701 - NEW YORK USA the whole document -----	1-12
A	HEIDRICH W ET AL: "AN IMAGE-BASED MODEL FOR REALISTIC LENS SYSTEMS IN INTERACTIVE COMPUTER GRAPHICS", PROCEEDINGS OF GRAPHICS INTERFACE '97. KELOWNA, BRITISH COLUMBIA, MAY 21 - 23, 1997; [PROCEEDINGS OF GRAPHICS INTERFACE], TORONTO, CIPS, CA, vol. CONF. 23, 21 May 1997 (1997-05-21), pages 68-75, XP000725342, ISBN: 978-0-9695338-6-3 abstract page 68, right-hand column, line 4 - line 9 page 69, right-hand column, line 1, paragraph 2.3 rendering thin lenses - page 71, left-hand column, last line, paragraph 3. An Image-BAsed Camera Model -----	1-12

-/--

C(Continuation).	DOCUMENTS CONSIDERED TO BE RELEVANT	
Category*	Citation of document, with indication, where appropriate, of the relevant passages	Relevant to claim No.
A	JIAZE WU ET AL: "Realistic rendering of bokeh effect based on optical aberrations", THE VISUAL COMPUTER ; INTERNATIONAL JOURNAL OF COMPUTER GRAPHICS, SPRINGER, BERLIN, DE, vol. 26, no. 6-8, 14 April 2010 (2010-04-14), pages 555-563, XP019845831, ISSN: 1432-2315 right-hand column, line 1, paragraph 1. Introduction - last line page 559, left-hand column, line 1, paragraph 5.1.2 - page 560, right-hand column, last line figure 6 -----	2-6
A	T. RITSCHEL ET AL: "Temporal Glare: Real-Time Dynamic Simulation of the Scattering in the Human Eye", COMPUTER GRAPHICS FORUM, vol. 28, no. 2, 1 April 2009 (2009-04-01), pages 183-192, XP55017598, ISSN: 0167-7055, DOI: 10.1111/j.1467-8659.2009.01357.x page 183, right-hand column, line 3, paragraph 1. Introduction - right-hand column, line 17 page 184, left-hand column, line 1 - line 12 page 184, right-hand column, line 36 - line 50 page 188, left-hand column, line 1, paragraph 5. Implementation - page 190, left-hand column, line 12 figures 1,6,8,9,10 -----	1-12
A	US 2005/270287 A1 (YASUTOMI KENICHIRO [JP]) 8 December 2005 (2005-12-08) figures 2,4,6,7,14 paragraph [0029] - paragraph [0032] paragraph [0036] - paragraph [0037] -----	1-12
A	US 7 206 725 B1 (ALSPACH TED [US]) 17 April 2007 (2007-04-17) the whole document -----	1-12
A	US 6 559 847 B1 (SEKI TAKUYA [JP]) 6 May 2003 (2003-05-06) column 1, line 22 - line 57 figures 2,8,10,13 -----	1-12

INTERNATIONAL SEARCH REPORT

Information on patent family members

Patent document cited in search report		Publication date	Patent family member(s)		Publication date
US 2005270287	A1	08-12-2005	JP	4479003 B2	09-06-2010
			JP	2005346429 A	15-12-2005
			US	2005270287 A1	08-12-2005
US 7206725	B1	17-04-2007	US	7206725 B1	17-04-2007
			US	7526417 B1	28-04-2009
			US	7974821 B1	05-07-2011
US 6559847	B1	06-05-2003	AU	7311900 A	17-04-2001
			BR	0013992 A	14-05-2002
			CA	2384603 A1	22-03-2001
			CN	1373884 A	09-10-2002
			DE	60001852 D1	30-04-2003
			DE	60001852 T2	22-01-2004
			EP	1214690 A1	19-06-2002
			MX	PA02002596 A	30-07-2002
			TW	472215 B	11-01-2002
			US	6559847 B1	06-05-2003
			WO	0120556 A1	22-03-2001